J|A|C|S
ARTICLES
Published on Web 07/30/2002

Silsesquioxane Models for Geminal Silica Surface Silanol Sites. A Spectroscopic Investigation of Different Types of Silanols

Tessa W. Dijkstra,[†] Robbert Duchateau,*[,‡] Rutger A. van Santen,[†] Auke Meetsma,[§] and Glenn P. A. Yap[⊥]

Contribution from the Schuit Institute of Catalysis and Department of Polymer Chemistry, Eindhoven University of Technology, P.O. Box 513, 5600 MB Eindhoven, The Netherlands, Crystal Structure Center, Chemical Physics, Material Science Center, University of Groningen, Nijenborgh 4, 9747 AG Groningen, The Netherlands, and Chemistry Department, University of Ottawa, K1N 6N5 Ottawa, Ontario, Canada

Received September 24, 2001

Abstract: The incompletely condensed monosilylated silsesquioxanes (c-$C_5H_9)_7Si_7O_9(OSiRR'_2)(OH)_2$ ($SiRR'_2$ = $SiMe_3$, $SiMe_2C(H)CH_2$, $SiMePh_2$) were reacted with $SiCl_4$ in the presence of an amine which yielded the dichloro compounds (c-$C_5H_9)_7Si_7O_9(OSiRR'_2)O_2SiCl_2$ (**1**−**3**). These compounds could be hydrolyzed into the corresponding silsesquioxanes containing geminal silanols, (c-$C_5H_9)_7Si_7O_9(OSiRR'_2)O_2Si(OH)_2$ (**4**−**6**). At elevated temperatures, the geminal silsesquioxanes **4** and **5** undergo condensation reactions and form the closed-cage silsesquioxane monosilanol, (c-$C_5H_9)_7Si_8O_{12}(OH)$. The more sterically hindered geminal silsesquioxane **6** undergoes in solution intermolecular dehydroxylation, yielding the thermodynamically stable dimeric disilanol, [(c-$C_5H_9)_7Si_7O_9(OSiMePh_2)(O_2Si(OH)$-)]$_2$-($\mu$-O) (**7**). NMR and FT-IR studies show that the two silanols of the geminal silsesquioxanes **4**−**6** are different from each other with respect to hydrogen bonding, both in solution and in the solid state. Hydrogen bonding of the geminal silanol-containing silsesquioxanes was examined and compared to hydrogen bonding in silsesquioxanes possessing vicinal or isolated silanol groups. The relative Brønsted acidity of the geminal silanols was determined using pK_{ip} (ion-pair acidity) measurements in THF with UV−vis. These acidities were compared with those of other silsesquioxanes containing silanol groups. Acidities of **4**−**6** were found to be among the lowest known for silsesquioxanes.

Introduction

Amorphous silicas play an important role in many different disciplines of chemistry. Siliceous materials are used, for instance, as absorbates and fillers[1,2] in acid-catalyzed reactions[3,4] or as catalyst supports.[5,6] Silica has unique properties and reactivity features, which stimulates ongoing research to gain a better understanding of the morphology, porosity, and surface characteristics of silica.[7] Molecular properties of silicas are strongly affected by the nature of their surface sites. The unsaturated surface valencies are satisfied by surface hydroxyl functionalities, which, depending on the calcination temperature, exist more or less as *vicinal* (hydrogen-bonded silanols), *geminal* (two silanol groups attached to the same silicon atom), or *isolated* (no hydrogen bonds possible) silanol sites (Figure 1).

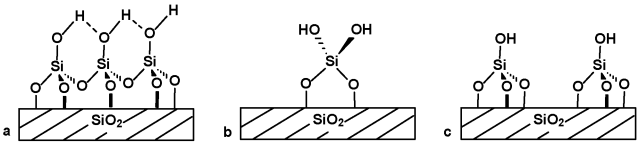

Figure 1. Schematic presentation of three types of silanol groups occurring on silica surfaces: (a) vicinal silanols, (b) geminal silanols, and (c) isolated silanols.

The molecular surface properties of porous silicious materials and zeolites are best studied by a combination of vibrational spectroscopy (i.e., Fourier transform IR, Raman, diffuse or total reflectance IR, and photoacoustic IR) and solid-state NMR spectroscopy that provides both qualitative and quantitative data.[8,9] However, these techniques are bulk measurements, and their sensitivity is often inadequate to obtain accurate data of

* Corresponding author. Tel.: +31-40-2474918. Fax +31-40-2455054. E-mail: R.Duchateau@tue.nl.
[†] Schuit Institute of Catalysis, Eindhoven University of Technology.
[‡] Department of Polymer Chemistry, Eindhoven University of Technology.
[§] University of Groningen.
[⊥] University of Ottawa.

(1) McCarthy, D. W.; Mark, I. E.; Schaefer, D. W. *J. Polym. Sci., Part B: Polym. Phys.* **1998**, *36*, 1167−1189.
(2) Choi, S.-S. *J. Appl. Polym. Sci.* **2001**, *79*, 1127−1133.
(3) Gorte, R. J. *Catal. Lett.* **1999**, *62*, 1−13.
(4) de Gauw, F. J. M. M.; van Santen, R. A. *Stud. Surf. Sci. Catal.* **2000**, *130A*, 127−135.
(5) Fink, G.; Steinmetz, B.; Zechlin, J.; Przybyla, C.; Tesche, B. *Chem. Rev.* **2000**, *100*, 1377−1390.
(6) Hlatky, G. G. *Chem. Rev.* **2000**, *100*, 1347−1376.
(7) Papirer, E. *Adsorption on Silica Surfaces*; Marcel Dekker: New York, 2000.
(8) Zhao, X. S.; Lu, G. Q.; Whittaker, A. K.; Millar, G. J.; Zhu, H. Y. *J. Phys. Chem. B* **1997**, *101*, 6525−6531.
(9) Morrow, B. A.; Gay, I. D. In *Adsorption on Silica Surfaces*; Papirer, E., Ed.; Marcel Dekker: New York, 2000; pp 9−33.

10.1021/ja0122243 CCC: $22.00 **© 2002 American Chemical Society**

local surface properties. Information on a molecular level is obtained either by indirect means of investigation (for instance, information gained from spectra before and after adsorption of an absorbate) or from computer simulations with the necessary simplifications to make the complex silica system manageable.[10,11] Recently, attempts have been made to synthesize well-defined molecular compounds to mimic certain silica surface sites. In this respect, silsesquioxanes and metallasilsesquioxanes are probably the most realistic homogeneous models for silica surface silanol and surface metal sites known to date.[12] An increasing number of these compounds have been prepared which resembled surface silanol sites (isolated and vicinal),[13,14] Lewis and Brønsted acidic surface sites,[15,16] or silica-grafted catalysts.[17] Because geminal silanols have not yet been modeled by silsesquioxanes, only spectroscopic data of simple organic silanediols could be used for studying geminal silica silanol sites.[18,19] Whereas the weak Brønsted acidity of surface silanols rarely affects catalytic reactions directly, a proper understanding of their chemical nature is essential for the preparation of supported catalysts. Protons of the surface hydroxyls ion-exchange readily with metal cations, a key step in catalyst preparation that should be related to the Brønsted acidity of the silanol functionality.

Here we report the synthesis of novel silsesquioxanes containing geminal silanols together with a detailed study on the thermal stability, solution and solid-state characteristics, and relative acidity of these compounds.

Results and Discussion

Synthesis of Geminal Silsesquioxanes Disilanols. For this study, monosilylated incompletely condensed silsesquioxanes of the type $(c\text{-}C_5H_9)_7Si_7O_9(OSiRR'_2)(OH)_2$ were used with sterically and electronically different silyl ether functionalities ($SiRR'_2$ = $SiMe_3$, $SiMe_2C(H)CH_2$, $SiMePh_2$). Reaction of these disilanols with an equimolar amount of silicon tetrachloride in the presence of 2 equiv of triethylamine afforded in high yield the geminal dichloro compounds $(c\text{-}C_5H_9)_7Si_7O_9(OSiRR'_2)O_2SiCl_2$ ($SiRR'_2$ = $SiMe_3$, **1**; $SiMe_2C(H)CH_2$, **2**; $SiMePh_2$, **3**). Compounds **1**−**3** readily hydrolyze, forming HCl and the corresponding geminal silanols $(c\text{-}C_5H_9)_7Si_7O_9(OSiRR'_2)O_2Si(OH)_2$ ($SiRR'_2$ = $SiMe_3$, **4**; $SiMe_2C(H)CH_2$, **5**; $SiMePh_2$, **6**; Scheme 1).

Both the geminal dichlorides (**1**−**3**) and the geminal silanols (**4**−**6**) show the expected pattern in the ^{13}C and ^{29}Si NMR spectra (respectively 1:1:2:2:1 and 1:1:2:1:2) for a C_s-symmetric structure (Figure 2). In addition, the ^{29}Si NMR spectra of **1**−**6** show silicon resonances characteristic for $(\equiv O)_2SiCl_2$ (± −68 ppm) and $(\equiv O)_2Si(OH)_2$ (± −89 ppm), respectively.[19] ^1H NMR shows that the two silanols of the geminal silsesquioxanes **4**−**6** are different in nature. Like the two chlorides in **1**−**3** (Figure 2), the silanols in **4**−**6** are exo and endo isomers with respect to the silyl ether functionality, and the hydroxyls occur as two distinct singlets in the proton NMR spectrum.

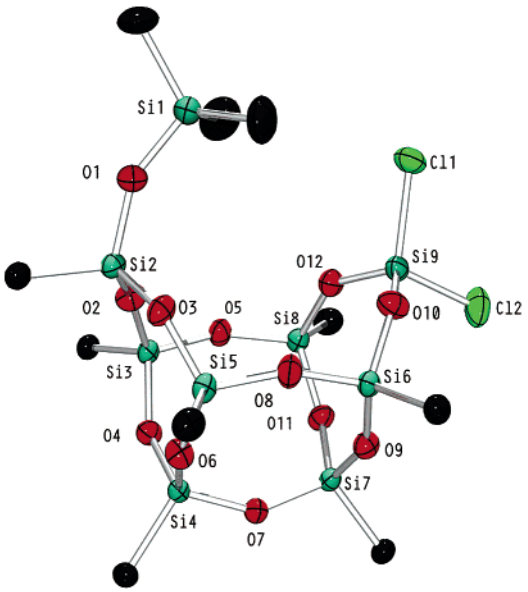

Figure 2. Molecular structure of $[(c\text{-}C_6H_{11})_7Si_7O_9(OSiMe_3)(O_2SiCl_2)]$ (**1′**). Thermal ellipsoids are scaled to enclose 40% of the electron density. Only the cyclohexyl methyne carbon is shown for clarity. Selected bond distances (Å): Si9−Cl1, 2.0303(11); Si9−Cl2, 2.0441(13); Si8−O12, 1.655(2); Si9−O10, 1.604(2); Si9−O12, 1.605(2); Si1−O1, 1.635(2); Si−O_{av}, 1.629(2). Angles (deg): Cl1−Si9−Cl2, 108.24(6); Cl1−Si9−O10, 107.72(9); Cl1−Si9−O12, 109.56(9); Cl2−Si9−O10, 109.65(10); Cl2−Si9−O12, 109.42(9); Si1−O1−Si2, 151.73(16); Si2−O2−Si3, 159.54(15); Si6−O10−Si9, 140.37(14); Si−O−Si_{av}, 149.90(14); O10−Si9−O12, 112.17(12); O5−Si8−O12, 106.54(12); O10−Si9−O12, 112.17(12); O−Si−O_{av}, 108.98(14).

Scheme 1. Synthesis of Geminal Silsesquioxanes Disilanols **4**−**6**

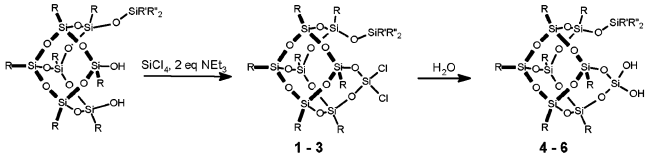

At elevated temperatures (80 °C), the geminal silsesquioxanes **4** and **5** are unstable and undergo intramolecular condensation to yield the closed-cage silsesquioxane monosilanol $(c\text{-}C_5H_9)_7Si_8O_{12}(OH)$ (Scheme 2). Compound **6** is infinitely stable in the solid state, even when exposed to elevated temperatures (80−120 °C). However, in solution, compound **6** slowly undergoes intermolecular dehydroxylation (even at room temperature), yielding the unprecedented siloxy-bridged dimeric bis(silanol), $[(c\text{-}C_5H_9)_7Si_7O_9(OSiMePh_2)(O_2Si(OH)\text{-})]_2\text{-}(\mu\text{-}O)$ (**7**). Interestingly, the condensation of **4** and **5** and the dehydroxylation of **6** proceed at much lower temperatures than for vicinal silsesquioxanes or on silica surfaces. Vicinal silsesquioxanes, $R_7Si_7O_9(OH)_2OR'$ (R = $c\text{-}C_5H_9$, $c\text{-}C_6H_{11}$; R′ = H, $SiMe_3$, $SbMe_4$), undergo dehydroxylation, affording the condensed $R_7Si_7O_{10}(OR')$. This reaction requires heating in the presence of molecular sieves (reflux in toluene) or a dehydrating agent such as O=PCl_3, $SbMe_5$, or MoO_2Cl_2.[12,14,20] For siliceous materials, calcination temperatures as high as 500 °C are needed to fully

(10) Sauer, J.; Ugliengo, P.; Garrone, E.; Saunders, V. R. *Chem. Rev.* **1994**, *94*, 2095−2160.
(11) Bródka, A. In *Adsorption on Silica Surfaces*; Papirer, E., Ed.; Marcel Dekker: New York, 2000; pp 243−276.
(12) Feher, F. J.; Budzichowski, T. A. *Polyhedron* **1995**, *14*, 3239−3253.
(13) Duchateau, R.; Abbenhuis, H. C. L.; van Santen, R. A.; Thiele, S. K.-H.; van Tol, M. F. H. *Organometallics* **1998**, *17*, 5222−5224.
(14) Feher, F. J.; Newman, D. A.; Walzer, J. F. *J. Am. Chem. Soc.* **1989**, *111*, 1741−1748.
(15) Duchateau, R.; Harmsen, R. J.; Abbenhuis, H. C. L.; van Santen, R. A.; Meetsma, A.; Thiele, S. K.-H.; Kranenburg, M. *Chem. Eur. J.* **1999**, *5*, 3130−3135.
(16) Edelmann, F. T.; Gun'ko, Y. K.; Giessman, S.; Olbrich, F. *Inorg. Chem.* **1999**, *38*, 210−211.
(17) Duchateau, R.; Cremer, U.; Harmsen, R. J.; Mohamud, S. I.; Abbenhuis, H. C. L.; van Santen, R. A.; Meetsma, A.; Thiele, S. K.-H.; van Tol, M. F. H.; Kranenburg, M. *Organometallics* **1999**, *18*, 5447−5459.
(18) Lickiss, P. D. *Adv. Inorg. Chem.* **1995**, *42*, 147−262.
(19) Wendler, C.; Reinke, H.; Kelling, H. *J. Organomet. Chem.* **2001**, *626*, 53−58.

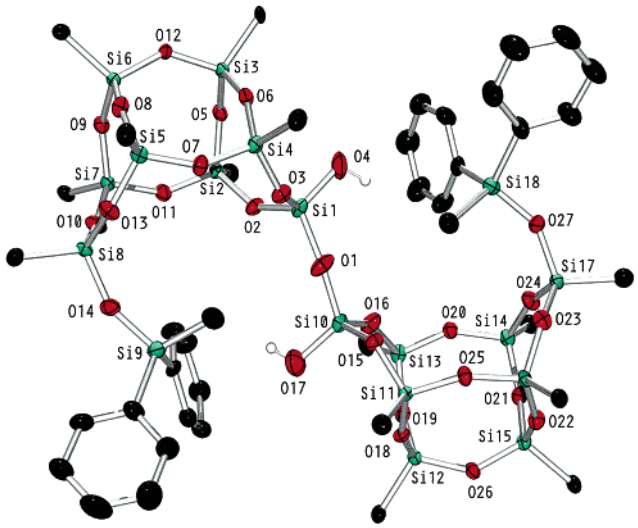

Figure 3. Molecular structure of $[(c\text{-}C_5H_9)_7Si_7O_9(OSiMePh_2)(O_2Si(OH)\text{-})]_2\text{-}(\mu\text{-}O)$ (**7**). Thermal ellipsoids are scaled to enclose 40% of the electron density. Only the cyclopentyl methyne carbon is shown for clarity. Selected bond distances (Å): Si1−O1, 1.604(4); Si1−O2, 1.613(4); Si1−O3, 1.619(4); Si1−O4, 1.618(4); Si10−O1, 1.596(4); Si10−O15, 1.618(4); Si10−O16, 1.594(4); Si10−O17, 1.609(5). Angles (deg): Si1−O1−Si10, 171.4(3); O1−Si1−O2, 108.8(2); O1−Si1−O3, 108.2(2); O1−Si1−O4, 112.1(2); O2−Si1−O3, 110.4(2); O2−Si1−O4, 109.6(2); O3−Si1−O4, 107.7(3); O1−Si10−O15, 108.8(2); O1−Si10−O16, 108.4(2); O1−Si10−O17, 112.8(3); O15−Si10−O16, 109.1(2); O15−Si10−O17, 107.3(2); O16−Si10−O17, 110.4(3).

Scheme 2. Thermal Behavior of **4**−**6**

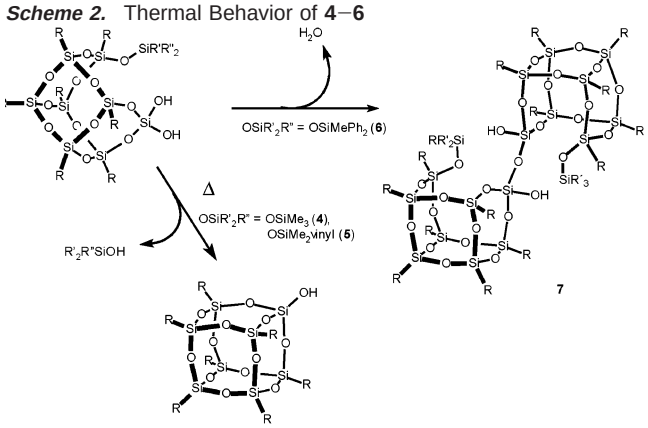

dehydroxylate the surface and form isolated silanols and condensed siloxane bonds.[21]

The molecular structures of **1′**[22] and **7**, determined by X-ray analyses, are shown in Figures 2 and 3, respectively. Compound **1′** is C_s symmetric, in which the two chlorides are exo- and endo-oriented with respect to the $SiMe_3$ silyl ether functionality. Si9 is tetrahedrally surrounded and, except for the slightly opened O10−Si9−O12 angle of 112.17(12)°, shows no signs of any strain or steric hindrance of the adjacent $SiMe_3$ silyl ether functionality. As expected for a more electrophilic silicon, the Si9−O10 (1.604(2) Å) and Si9−O12 (1.605(2) Å) are significantly shorter than the average Si−O distance of 1.629(2) Å and result in elongation of the corresponding Si6−O10 (1.645(2) Å) and Si8−O12 (1.655(2) Å) distances. Compound **7** consists of two silsesquioxane fragments linked together by a bridging oxygen atom. The Si1−O1−Si10 angle of 171.4(2)° is nearly linear, and O1 roughly forms the inversion center of the molecule. Similar to the observation for the electrophilic Si9 in **1′**, the lack of an electron-donating cycloalkyl group at Si1 and Si10 results in significantly shorter Si−O distances (av. 1.609(4) Å) than the average distance (1.628(4) Å) of the other Si−O bonds in **7**, which are within the wide range of Si−O distances known for silsesquioxanes.

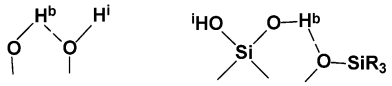

Figure 4. Isolated (H^i) and hydrogen-bonded (H^b) types of silanols.

Solid-State and Solution Properties of Geminal Silsesquioxane Silanols. To study silica surface properties such as hydrogen bonding, relative acidity, or dehydroxylation reactions of various silanols, the infrared stretching vibrations (ν_{OH}) of the surface silanols are very informative. These bands are well-separated from other vibrations and are largely dependent on interactions with neighboring silanols, silyl ethers, or metal species. For silica, a broad absorption around 3530 cm^{-1} (vacuum) is usually assigned to hydrogen-bonded silanols close to other silanols acting as a proton acceptor. Absorptions around 3750 cm^{-1} (vacuum) have been assigned to isolated silanols (Figure 4). Stretching vibrations of geminal silanols are usually found in the same region as isolated silanols, and still controversy exists about whether they can be distinguished separately.[23,24] Interestingly, Takei and co-workers[25] reported an additional shoulder at 3600 cm^{-1}, suggesting both hydrogen-bonded and isolated geminal silanols. Boccuzzi and co-workers found the same phenomenon on silica at low temperatures.[26] Infrared spectroscopy studies on geminal silsesquioxane disilanols could give more insight into the possible vibrations of geminal silanols.

When comparing the solid-state and solution IR spectra of silsesquioxanes with the IR spectra of silica surface silanols measured in a vacuum, one should ensure that the medium used to record the IR spectra of the samples does not affect the silanol frequencies. Solid-state FT-IR spectra of silsesquioxanes recorded using Nujol mulls are identical to those collected using an ATR (golden gate) device, indicating that Nujol shows no significant interaction with the silanols. Nujol mulls were preferred as they gave better-resolved silanol stretching vibrations than the ATR device; solution IR spectra were recorded in CCl_4. The observed frequencies for silsesquioxanes bearing isolated silanols are close to the value of 3750 cm^{-1} for isolated silica surface silanols in vacuum, indicating that the interaction of CCl_4 with silanols is negligible. This is in agreement with early work of Hair and Hertl on the effect of different solvents on silica−silanol frequencies, which showed that CCl_4 gives only a small shift of 45 cm^{-1} compared to the value in vacuum, whereas diethyl ether gives a shift of 430 cm^{-1}.[27] As expected, when diethyl ether was added to the CCl_4 solutions of

(20) Feher, F. J.; Budzichowski, T. A.; Rahimian, K.; Ziller, J. W. *J. Am. Chem. Soc.* **1992**, *114*, 3859−3866.
(21) Morrow, B. A.; McFarlan, A. J. In *The Colloid Chemistry of Silica*; Bergna, H. E., Ed.; American Chemical Society: Washington, DC, 1994; pp 183−198.
(22) Only **1′**, the cyclohexyl-substituted analogue of **1**, gave crystals suitable for an X-ray analysis.
(23) van Roosmalen, A. J.; Mol, J. C. *J. Phys.Chem.* **1978**, *82*, 2748.
(24) Hoffmann, P.; Knozinger, E. *Surf. Sci.* **1987**, *188*, 181.
(25) Takei, T.; Kato, K.; Meguro, A.; Chikazawa, M. *Colloids Surf. A* **1999**, *150*, 77−84.
(26) Ghiotti, G.; Garrone, E.; Morterra, C.; Boccuzzi, F. *J. Phys. Chem.* **1979**, *83*, 2863.
(27) Hair, M. L.; Hertl, W. *J. Chem. Phys.* **1970**, *74*, 91−94.

Table 1. Comparative NMR Resonances and IR Vibrations of the Geminal Silanols **4**−**6**

compd	^{1}H NMR (ppm) δ Si(OH)$_2$	^{29}Si NMR (ppm) δ Si(OH)$_2$	IR (Nujol) ν_{OH} (cm^{-1})	IR (CCl_4) ν_{OH} (cm^{-1})	IR (CCl_4 + Et_2O) ν_{OH} (cm^{-1})	pK_{ip}[a]
4	2.41, 3.80	−89.43	3515, 3402	3700, 3584	3374	10.2 ± 0.1
5	2.37, 3.63	−89.45	3520, 3402	3700, 3591	3373	10.1 ± 0.1
6	2.12, 2.23	−89.46	3582, 3438	3699, 3625	3373	9.7 ± 0.3

[a] pK_{ip} averages of two indicators, Li$^+$[9-(cyano)fluorenide]$^-$·2THF and Li$^+$[9-(methoxycarbonyl)fluorenide]$^-$·2THF.

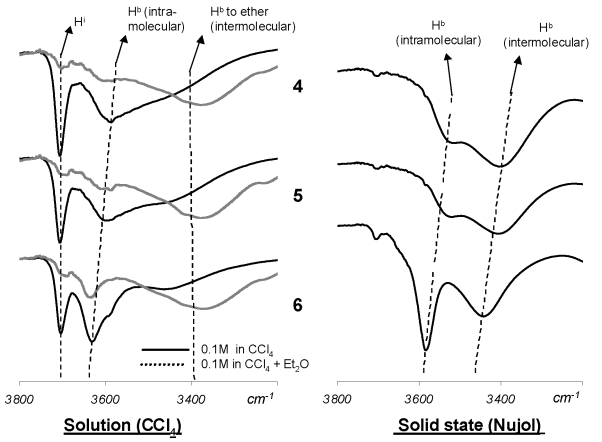

Figure 5. OH vibrations of the IR spectra of **4**−**6** in the solid state (Nujol) and in solution (CCl_4 and CCl_4 + Et_2O). Different hydrogen bonding types are indicated: isolated (H^i), intramolecular or intermolecular hydrogen bonded (H^b).

silsesquioxanes, all silanols become hydrogen-bonded (broad vibration around 3375 cm^{-1}) as a result of the strong interaction of the ether with silsesquioxane silanols.

FT-IR spectroscopy studies on **4**−**6** revealed that both hydroxyl groups in **4**−**6** are different in nature not only due to their geometric inequivalency, but also with respect to hydrogen bonding. Moreover, the hydroxyl groups are differently bonded in solution and in the solid state. The infrared OH stretching vibrations of CCl_4 solutions of **4**−**6** appear as one broad and one sharp signal (Table 1, Figure 5). The sharp signal at 3700 cm^{-1} is indicative for isolated silanols. The broad vibration around 3600 cm^{-1} is characteristic for a hydrogen-bonded silanol. Interestingly, in the solid-state IR spectra (Nujol), no isolated silanol vibrations are observed. Instead, two broad vibration bands are found. The broad vibration band at 3600 cm^{-1} corresponds with the vibration of the hydrogen-bonded silanol in solution. The broad vibration at 3400 cm^{-1} is also indicative for a hydrogen-bonded silanol but is clearly of a different type than the former one. Any possible weak interaction of CCl_4 with silanol functionalities cannot account for these striking differences observed for the solid-state (Nujol) and solution (CCl_4) infrared spectra.

Small organic molecules bearing vicinal or geminal silanols have been found to form intermolecularly poly-hydrogen-bonded networks in the form of ladder-like chains,[28,29] sheets,[30] layers,[31] or more three-dimensional solid-state structures.[32] Tilley and co-workers[33] found for a tetrahydroxydisiloxane both intramolecular and intermolecular hydrogen bonds. They demonstrated that a pendant silyl ether functionality can act as proton acceptor, giving rise to the intramolecular hydrogen bonds (Figure 4) that show a broad OH stretching vibration band at 3438 cm^{-1} (solid state, KBr) in the FT-IR spectrum.

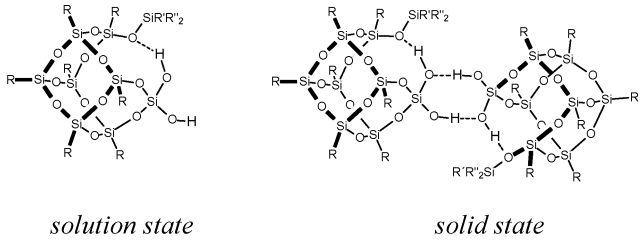

Figure 6. Proposed solution and solid-state structures of **4**−**6**.

To better predict the solution structures of **4**−**6**, molecular weight measurements in benzene were carried out, which showed that all three geminal silsesquioxane silanols **4**−**6** are monomeric in solution. On the basis of the similar hydrophobicity of both solvents (benzene, ϵ = 2.3; CCl_4, ϵ = 2.2 at 20 °C),[34] **4**−**6** are assumed to be monomeric in CCl_4 as well. On the other hand, preliminary results of a single-crystal X-ray analysis show that the structure of **4** is dimeric in the solid state.[35] On the basis of their monomeric structure in solution, the observed hydrogen bonding of **4**−**6** in solution is most probably an intramolecular interaction of the *endo*-silanol with the silyl ether functionality, comparable to the observed intramolecular interaction observed by Tilley (Figure 6). Manners and co-workers investigated the hydrogen bonding of diferrocenylsilanediol both in solution (CCl_4) and in the solid state.[36] As for **4**−**6**, in solution one sharp signal is found at approximately 3700 cm^{-1}, suggesting isolated silanols and thus logically the existence of monomers. However, in the solid state, only broad vibration bands around 3400 cm^{-1} were observed. Supported by an X-ray structure analysis, the vibration bands could be subscribed to hydrogen bonding of one of the silanols to another molecule, thus forming dimeric structures, while the other silanol group forms a hydrogen bond to a neighboring dimer. These findings support the proposed intramolecular hydrogen bonds to the silyl ether functionality in the monomeric solution structures of **4**−**6**, as well as the intra- and intermolecular hydrogen bonding in the dimeric solid-state structures of compounds **4**−**6**. Yet in the case of geminal silsesquioxanes, the silanol not participating in intermolecular hydrogen bonding is more likely to form intramolecular hydrogen bonds to the pendant silyl ether functionality than to a neighboring dimer, as found for the diferrocenylsilanediol (Figure 6).

(28) Buttrus, N. H.; Eaborn, C.; Hitchcock, P. B.; Lickiss, P. D.; Taylor, A. D. *J. Organomet. Chem.* **1986**, *309*, 25−33.
(29) Buttrus, N. H.; Eaborn, C.; Hitchcock, P. B.; Saxena, A. K. *J. Organomet. Chem.* **1985**, *284*, 291−297.
(30) Lickiss, P. D.; Litster, S. A.; Redhouse, A. D.; Wisener, C. J. *J. Chem. Soc., Chem. Commun.* **1991**, 173−174.
(31) Tomlins, P. E.; Lydon, J. E.; Akrigg, D.; Sheldrick, B. *Acta Crystallogr., Sect. C* **1985**, *41*, 941.
(32) Carré, F.; Cerveau, G.; Corriu, R. J. P.; Dabiens, B. *J. Organomet. Chem.* **2001**, *624*, 354−358.
(33) Rulkens, R.; Coles, M. P.; Tilley, T. D. *J. Chem. Soc., Dalton Trans.* **2000**, 627−628.
(34) *Handbook of Chemistry and Physics*; CRC Press: Boca Raton, FL, 1991.
(35) Evans, J., personal communication at SHHC10 symposium, July 2001, Lyon, France.
(36) MacLachlan, M. J.; Ginzburg, M.; Zheng, J.; Knöll, O.; Lough, A. J.; Manners, I. *New J. Chem.* **1998**, 1409−1415.

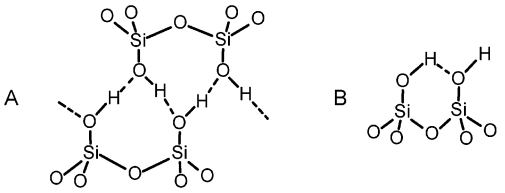

Figure 7. Poly-hydrogen-bonded silanols (A) and mono-hydrogen-bonded silanols (B).

When comparing the vibration bands of the hydrogen-bonded silanols of **4** and **6** in CCl_4 solution, hydrogen bonding for compound **4** is strongest because the vibration band shows the strongest shift to lower frequencies (a shift of 41 cm^{-1} compared to **6**). Proton NMR data supports this, as the $\Delta\delta$ of the two hydroxyls in **4** (1.39 ppm) is significantly larger than the $\Delta\delta$ observed for compound **6** (0.11 ppm). From IR and NMR, it is clear that the hydrogen bonding in **5** ($\Delta\nu$ is 109 cm^{-1} and $\Delta\delta$ is 1.26 ppm) is slightly less than that in compound **4** but still considerably stronger than that in **6**. This difference in hydrogen bonding for **4** and **6** in solution is probably due to both steric and electronic reasons. The $SiMe_3$ group in **4** is sterically less bulky than the $SiMePh_2$ group in **6**, while it is also the most electron donating one and therefore more able to stabilize the hydrogen-bonded proton. A similar phenomenon was observed in the Brønsted acidic aluminosilsesquioxanes $\{[(c\text{-}C_5H_9)_7Si_7O_{11}(OSiMe_3)]_2Al\}^-H^+$ and $\{[(c\text{-}C_5H_9)_7Si_7O_{11}(OSiMePh_2)]_2Al\}^-H^+$. The bulkier and less electron donating $SiMePh_2$ substituent in the latter hampers intramolecular hydrogen bonding and renders the complex more acidic than the $SiMe_3$-substituted complex.[37]

The observed difference in hydrogen bonding for **4** and **5** versus **6** most probably is responsible for the different thermal condensation reactions. The effective intramolecular hydrogen bonds with the pendant silyl ether functionality in **4** and **5** might promote the intramolecular condensation into a closed caged structure. The reduced capacity of the bulky, poor electron donating silyl ether functionality of **6** makes intramolecular hydrogen bonding less preferable, and consequently intermolecular dehydroxylation is favored (Scheme 2).

Comparison of Different Types of Silsesquioxane Silanols. Due to their well-defined structures, silsesquioxanes are suitable complexes for understanding electronic and vibrational structures of zeolite and silicate frameworks.[38,39] A combined spectroscopic (FTIR) and computational study (DFT) showed that silsesquioxanes containing silanols are excellent tools to clarify the infrared hydroxyl bands of hydroxyl nests found in zeolites.[40] With the availability of geminal silanols, a full comparison of the three types of silanol groups occurring in incompletely condensed silsesquioxanes is now possible. Poly- and mono-hydrogen-bonded silanol sites can clearly be distinguished; vibration bands for poly-hydrogen-bonded silanols are situated around 3200 cm^{-1}, whereas mono-hydrogen-bonded silanols are found in the 3400−3600 cm^{-1} range, depending on the effectiveness of the bonding (Figure 7). These values correspond well with the stretching vibration bands of the poly-hydrogen-bonded $(c\text{-}C_7H_{13})_7Si_6O_7(OH)_4$ and $(c\text{-}C_6H_{11})_7Si_7O_9(OH)_3$ and the intermolecular mono-hydrogen-bonded silanols in the solid-state structures of **4** and **6** (Figure 6). Crystal structure determinations proved that not only $(c\text{-}C_7H_{13})_7Si_6O_7(OH)_4$ and $(c\text{-}C_6H_{11})_7Si_7O_9(OH)_3$ but also $(c\text{-}C_5H_9)_7Si_7O_9(OSiR'_3)(OH)_2$ (SiR'_3 = $SiMe_3$, $SiMePh_2$) are poly-hydrogen-bonded, dimeric structures in the solid state, which corresponds well with the observed stretching vibrations ranging from 3200 to 3300 cm^{-1}.

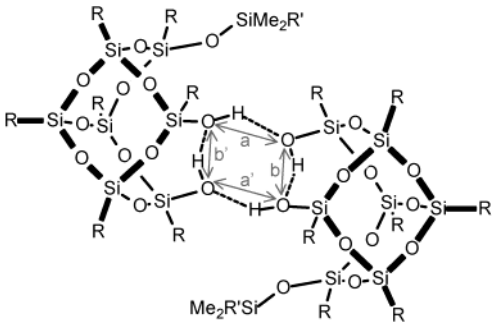

Figure 8. Solid-state configuration of mono-silylated silsesquioxanes with vicinal silanol groups. Intramolecular silanol−oxygen distances are depicted with *b* and *b′*, intermolecular silanol−oxygen distances with *a* and *a′*.

Table 2. Intermolecular (*a*, *a′*) and Intramolecular Silanol−Oxygen Distances (*b*, *b′*) for Three Different Monosilylated Silsesquioxanes

	a	*a′*	*b*	*b′*
$(c\text{-}C_6H_{11})_7Si_7O_9(OSiMe_2Ph)(OH)_2$	2.670	2.670	2.722	2.722
$(c\text{-}C_5H_9)_7Si_7O_9(OSiMe_2{}^tBu)(OH)_2$	2.694	2.748	2.639	2.708
$(c\text{-}C_5H_9)_7Si_7O_9(OSiMe_3)(OH)_2$	2.663	2.659	2.692	2.684

While the vicinal tri- and tetrasilanols also form strongly hydrogen-bonded dimeric structures in solution, the vicinal disilanols $(c\text{-}C_5H_9)_7Si_7O_9(OSiR'_3)(OH)_2$ (SiR'_3 = $SiMe_3$, $SiMePh_3$) are less effectively hydrogen bonded in solution, which is accompanied with a shift of the silanol stretching vibration to almost 3500 cm^{-1} (Figure 8). Interestingly, the solution IR spectrum of the vicinal disilanol $(c\text{-}C_5H_9)_7Si_7O_9(OSiMePh_2)(OH)_2$ shows two distinct hydroxyl vibrations. The reason for this phenomenon can be found in the large steric bulk of the $SiMePh_2$ substituent. Crystal structure data of mono-silylated silsesquioxanes bearing two vicinal silanols reveal that the molecules form bridged dimers via silanol hydrogen bonds (Figure 8) with a symmetry close to C_{2v}. In Table 2, intra- and intermolecular oxygen distances of the four silanols groups are displayed for three different silsesquioxane compounds, $(c\text{-}C_6H_{11})_7Si_7O_9(OSiMe_2Ph)(OH)_2$[41] and $(c\text{-}C_5H_9)_7Si_7O_9(OSiMe_2R)(OH)_2$ (R = Me,[42] t-Bu[43]).

As can be seen in Table 2, when going from a small silyl ether functionality (i.e., $SiMe_3$) to a bulkier group (i.e., $SiMe_2{}^tBu$ or $SiMe_2Ph$), the difference in distances between intramolecular silanol−oxygen and intermolecular silanol−oxygen becomes larger. This indicates that a bulkier group distorts the symmetry of the hydrogen-bonded $[OH]_4$ core somewhat. When these observations are extrapolated to the bulky $OSiMePh_2$ silyl ether functionality, one would expect increased distortion or even prevention of formation of the $[OH]_4$ core, as shown in

(37) Skowronska-Ptasinska, M. D.; Duchateau, R.; van Santen, R. A.; Yap, G. P. A. *Eur. J. Inorg. Chem.* **2001**, 133−137.
(38) Davidova, I. E.; Gribov, L. A.; Maslov, I. V.; Dufaud, V.; Niccolai, G. P.; Bayard, F.; Basset, J.-M. *J. Mol. Struct.* **1998**, *443*, 89−106.
(39) Marcolli, C.; Laine, P.; Buhler, R.; Calzaferri, G. *J. Phys. Chem. B* **1997**, *101*, 1171−1179.
(40) Krijnen, S.; Harmsen, R. J.; Abbenhuis, H. C. L.; van Hooff, J. H. C.; van Santen, R. A. *Chem. Commun.* **1999**, 501−502.
(41) Feher, F. J.; Newman, D. A. *J. Am. Chem. Soc.* **1990**, *112*, 1931−1936.
(42) Abbenhuis, H. C. L.; Burrows, A. D.; Kooijman, H.; Lutz, M.; Palmer, M. T.; van Santen, R. A.; Spek, A. L. *Chem. Commun.* **1998**, 2627−2628.
(43) Arnold, P. L.; Blake, A. J.; Hall, S. N.; Ward, B. D.; Wilson, C. *J. Chem. Soc., Dalton Trans.* **2001**, 488−491.

Table 3. Comparison of Acidity of Vicinal, Geminal, and Isolated Silanol Groups.

type of silanol	compound	pK_{ip}[a]	IR (Nujol) ν_{OH} (cm^{-1})	IR (CCl_4) ν_{OH} (cm^{-1})	IR (CCl_4 + Et_2O) ν_{OH} (cm^{-1})
vic. tetrasilanol	$(c\text{-}C_7H_{13})_7Si_6O_7(OH)_4$	7.5 ± 0.2	3183	3225	3225
vic. trisilanol	$(c\text{-}C_6H_{11})_7Si_7O_9(OH)_3$	7.6 ± 0.2	3158	3217	3217
vic. disilanol	$(c\text{-}C_5H_9)_7Si_7O_9(OSiMe_3)(OH)_2$	9.5 ± 0.1	3261	3471	3415
	$(c\text{-}C_5H_9)_7Si_7O_9(OSiMePh_2)(OH)_2$	9.9 ± 0.2	3327	3592, 3453	3416
gem. disilanol	4	10.2 ± 0.1	3515, 3402	3700, 3584	3374
	6	9.7 ± 0.3	3582, 3438	3699, 3625	3373
mono silanol	7		3629	3626	3391
	$(c\text{-}C_5H_9)_7Si_8O_{12}(OH)$	8.9 ± 0.4	3706, 3444	3700	3348
	$(c\text{-}C_5H_9)_7Si_7O_9(O_2SiMe_2)OH$	9.6 ± 0.4	3564	3549	3417

[a] pK_{ip} averages of two indicators, Li^+[9-(cyano)fluorenide]$^-$·2THF and Li^+[9-(methoxycarbonyl)fluorenide]$^-$·2THF.

Figure 8. Clearly, this effect will be largest in solution, which explains the two distinct vibrations in the solution infrared spectrum: one signal around 3600 cm^{-1}, indicative for an intramolecular hydrogen bond to the silyl ether functionality, and one signal around 3450 cm^{-1}, indicative for an intramolecular mono-hydrogen bond (Figure 4).

In solution, the silanol group of the fully condensed $(c\text{-}C_5H_9)_7Si_8O_{12}(OH)$ is truly isolated (3700 cm^{-1}), whereas in the solid state also an intermolecularly mono-hydrogen-bonded vibration occurs at 3450 cm^{-1}. The latter vibration, indicative for a dimeric structure, most probably corresponds to the crystalline phase. For the monosilanol compound containing a small additional intramolecular electron-donating siloxane ring $(c\text{-}C_5H_9)_7Si_7O_9(O_2SiMe_2)OH$[44] (Table 3), the silanol vibration is shifted toward lower frequencies (around 3550 cm^{-1} in solution as well as in the solid state). This shift can be explained by intramolecular interaction with the additional siloxane ring. The condensed compound **7** is a somewhat special case; both silanols show the same amount of intramolecular bonding in solution and in the solid state (3626 and 3629 cm^{-1} respectively). Because of the steric bulk of **7**, interaction with other molecules is effectively prevented, and no differences can be expected between the compound in solution and the compound in the solid state (Table 3, Figure 9).

Relative Brønsted Acidities of Different Types of Silsesquioxane Silanols. Whereas the weak Brønsted acidity of silica surface silanols rarely affects catalytic reactions directly, a proper understanding of the chemical nature of silica surface silanols is essential for the preparation of silica-supported catalysts. Since the protons of the surface hydroxyls ion-exchange readily with metal cations, there should be a relationship between the ion-exchange rate and the Brønsted acidity of the silanol functionalities. It is important to recognize at this point that acidities are strongly solvent dependent. The dissociation constant of an acid depends on the ability of the solvent to solvate the proton, the anion, and the undissociated acid. The silsesquioxanes used in this study are highly lypophilic and dissolve only in organic solvents with relatively low polarity like THF or hexane. In solvents with a relatively low dielectric constant such as THF ($\epsilon_{(25°C)} = 7.4$), ion-pair dissociation hardly occurs.[45−49] Hence, acidity measurements in low-polarity solvents give only qualitative values of relative acidities in each specific solvent; i.e., one can only determine whether one compound is more or less acidic than another one in a specific solvent. However, this qualitative information is still very significant for ion-exchange reactions and thus for the synthesis of supported catalysts.

Using the overlapping indicator method,[17,41] acidity measurements in THF afford relative ion-pair acidities for the various silsesquioxane silanols. When comparing the ion-pair acidity of the closed-cage silsesquioxane containing an isolated silanol $(c\text{-}C_5H_9)_7Si_8O_{12}(OH)$ (pK_{ip} = 8.9) with that of the monosilanol compound $(c\text{-}C_5H_9)_7Si_7O_9(O_2SiMe_2)OH$ (pK_{ip} = 9.6, Table 3), the latter compound appears to be less acidic as a result of the electron-donating effect of the additional intramolecular siloxane ring. Deprotonation NMR experiments on an equimolar mixture of $(c\text{-}C_5H_9)_7Si_8O_{12}(OH)$, $(c\text{-}C_5H_9)_7Si_7O_9(O_2SiMe_2)OH$, and one of the indicators used for the pK_{ip} determinations in THF-d_8 (Li^+[9-(cyano)fluorenide]$^-$·2THF) indeed showed a clear preference for deprotonation of the former. The differences in ion-pair acidity for geminal (**4**−**6**) and corresponding vicinal disilanols $(c\text{-}C_5H_9)_7Si_7O_9(OSiR'_3)(OH)_2$ (SiR'_3 = $SiMe_3$, $SiMePh_3$) are small. Vicinal tetra- and trisilanol-containing silsesquioxanes are much more acidic than all other silanols. Calorimetric adsorption experiments by Drago and Chronister[50] nicely demonstrated that poly-hydrogen-bonded silanols (Figure 7) give rise to very effective hydrogen bonding, which generally results in more acidic systems than mono-hydrogen-bonded silanols. As could be seen from the IR data, silsesquioxanes containing vicinal tri- and tetrasilanols are capable of poly-hydrogen bonding even in solution, while silsesquioxanes containing vicinal disilanols give considerably less effective hydrogen bonding in solution (Figure 9). Consequently, the tetra- and trisilanols $(c\text{-}C_7H_{13})_7Si_6O_7(OH)_4$ and $(c\text{-}C_6H_{11})_7Si_7O_9(OH)_3$ are up to 3 orders of magnitude more acidic than the vicinal disilanols $(c\text{-}C_5H_9)_7Si_7O_9(OSiR'_3)(OH)_2$ (SiR'_3 = $SiMe_3$, $SiMePh_2$; Table 3). This difference in acidity of the trisilanol $(c\text{-}C_6H_{11})_7Si_7O_9(OH)_3$ and the disilanol $(c\text{-}C_6H_{11})_7Si_7O_9(OSiMe_3)(OH)_2$ was nicely demonstrated by Feher and Newman, who found that silylation of $(c\text{-}C_6H_{11})_7Si_7O_9(OH)_3$ is 4 orders of magnitude faster than that of $(c\text{-}C_6H_{11})_7Si_7O_9(OSiMe_3)(OH)_2$.[41]

Monitoring the interaction of silanols with external Lewis bases by IR spectroscopy is a common method to determine silica surface silanol acidities.[51] In the presence of a proton acceptor such as diethyl ether, the ν_{OH} vibrations shift as a result

(44) $(c\text{-}C_5H_9)_7Si_7O_9(O_2SiMe_2)OH$ was prepared by a method similar to that used for the Me_2Si-bridged silsesquioxanes derivative $[(c\text{-}C_6H_{11})_7Si_7O_9(OSiMe_2O)]_2(OSiMe_2O)$ (Lorenz, V.; Spoida, M.; Fischer, A.; Edelmann, F. T. *J. Organomet. Chem.* **2001**, *625*, 1−6) by treatment of $(c\text{-}C_5H_9)_7Si_7O_9(OH)_3$ with an equimolar amount of Me_2SiCl_2 and 2 equiv of NEt_3.

(45) Fachetti, A.; Kim, Y.-J.; Streitweiser, A. J. *J. Org. Chem.* **2000**, *65*, 4195−4197.

(46) Streitweiser, A. J.; Kim, Y.-J. *J. Am. Chem. Soc.* **2000**, *122*, 11783−11786.

(47) Cooksen, R. F. *Chem. Rev.* **1974**, *74*, 5−28.

(48) Bordwell, F. *Acc. Chem. Rev.* **1988**, *21*, 456−463.

(49) Kaufman, M. J.; Streitweiser, A. J. *J. Am. Chem. Soc.* **1987**, *109*, 6097.

(50) Chronister, C. W.; Drago, R. S. *J. Am. Chem. Soc.* **1993**, *115*, 4793−4798.

(51) Badger, R. M.; Bauer, S. H. *J. Chem. Phys.* **1937**, *5*, 839−851.

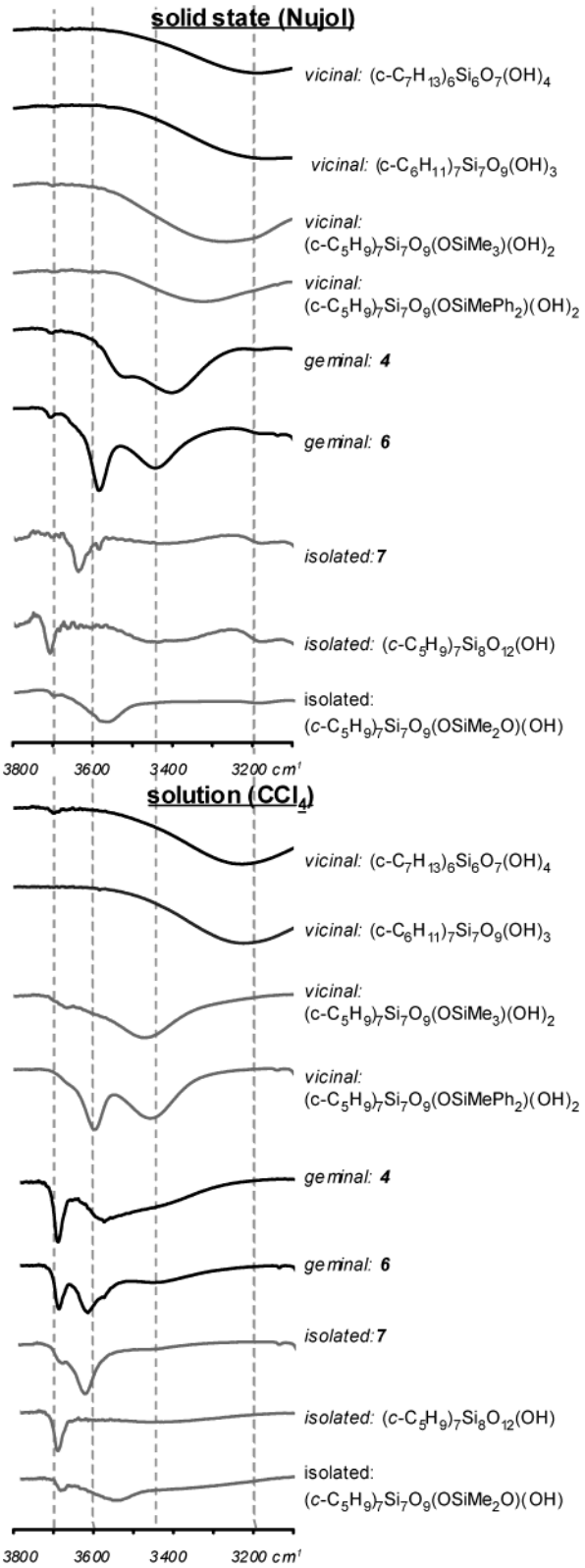

Figure 9. IR stretching vibrations of various silanols in solid state (Nujol) and solution (CCl_4). Several types of hydrogen bonding can be distinguished: isolated (±3700 cm^{-1}), intramolecular hydrogen-bonded (±3600, ±3450 cm^{-1}), intermolecular hydrogen bonded (±3400 cm^{-1}), and poly-hydrogen-bonded (3200 cm^{-1}).

of hydrogen bonding between the silanol and the ether. Indeed, when ether is added to tetrachloromethane solutions of **4**−**6**, the two distinct vibration bands are replaced by a broad hydrogen-bonded band (Figure 5, Table 1). Adding ether to tetrachloromethane solutions of silsesquioxanes with vicinal disilanols or isolated silanols results in a hydrogen-bonded vibration band at comparable frequencies (Table 3). The strong dimeric structures of silsesquioxanes containing vicinal tri- and tetrasilanols are not noticeably affected when ether is added to the tetrachloromethane solutions. These findings confirm the earlier conclusion that silsesquioxanes capable of poly-hydrogen bonding are dimeric both in the solid state and in solution. However, differences in OH vibration shifts as a result of adding ether to the silsesquioxanes solutions are too small to be used as a probe for relative Brønsted acidities of the investigated silsesquioxanes silanols. The relative ion-pair acidities obtained by the overlapping method proved to be much more valuable.

Conclusion

Silsesquioxanes containing geminal silanols of the type (*c*-$C_5H_9)_7Si_7O_9(OSiR'_3)O_2Si(OH)_2$ are readily accessible by reaction of the incompletely condensed silsesquioxanes (*c*-$C_5H_9)_7Si_7O_9(OSiR'_3)(OH)_2$ with $SiCl_4$ in the presence of an amine, followed by hydrolysis. NMR and FT-IR studies show that the two silanols of the geminal silsesquioxanes are different in nature. In solution, one of the silanols is intramolecularly hydrogen bonded while the other is isolated. In the solid state, both silanols are hydrogen bonded, one intramolecularly and the other intermolecularly. At elevated temperatures, the geminal silsesquioxanes with silyl ether functionalities that are best capable of stabilizing the intramolecular hydrogen bond ($OSiMe_3$ and $OSiMe_2C(H)CH_2$) undergo condensation reactions, yielding the closed-cage silsesquioxane monosilanol (*c*-$C_5H_9)_7Si_8O_{12}(OH)$. In solution, the geminal silsesquioxane with a bulkier and less electron donating $OSiMePh_2$ substituent and therefore diminished hydrogen bonding is more inclined to form the thermodynamically stable intermolecular dehydroxylation product, [(*c*-$C_5H_9)_7Si_7O_9(OSiMePh_2)(O_2Si(OH)$-)]$_2$-($\mu$-O). With the availability of geminal silanols, a full comparison of the three types of silanol groups occurring in incompletely condensed silsesquioxanes could be made. Ion-pair acidity measurements in THF show that geminal silanols are among the least acidic incompletely condensed silsesquioxanes and readily undergo dehydroxylation or condensation reactions. For multiple vicinal hydroxyl groups, intermolecular poly-hydrogen bonding both in solution and in the solid state is clearly favored. When interactions of silanols with each other become sterically hampered, intramolecular hydrogen bonding with adjacent silyl ether functionalities is often observed.

Experimental Section

General Remarks. Reactions were performed under an argon atmosphere using Schlenk techniques when necessary. Solvents were distilled from K (THF), Na/K alloy (hexanes, C_6D_6), and Na-benzophenon-ketyl (Et_2O) or dried over 4 Å molecular sieves (NEt_3, CCl_4, $CDCl_3$, THF-d_8) and stored under argon. ^1H and ^{13}C NMR spectra were recorded on Varian Mercury 400 spectrometers (25 °C, ^1H NMR at 400 MHz, ^{13}C NMR at 100.6 MHz). ^{29}Si NMR spectra were recorded on a Varian Indigo 500 spectrometer (25 °C, 99.3 MHz). Chemical shifts are reported in ppm and referenced to residual solvent resonances (^1H, ^{13}C NMR) or external standards (^{29}Si, $SiMe_4 = 0$ ppm). All Fourier-transformed infrared spectra were recorded at room temperature on a Nicolet Avatar 360 spectrophotometer. Samples in solution were prepared under an inert atmosphere (glovebox). ν_{OH} values were determined in 0.1 M CCl_4 solutions and ν_{OH} in 0.1 M CCl_4 solutions

containing 0.25 M diethyl ether. Solid-state samples were recorded as Nujol mulls (prepared under an inert atmosphere, glovebox) or recorded directly on a Nicolet Smart DuraSamplIR in air for single-reflection diamond ATR analysis (golden gate). UV−vis measurements for determination of the pK_{ip} values were performed on a UV-2401PC spectrophotometer with standard slit width and scan speed. Molecular weight determinations in benzene were performed in the laboratory of Prof. J. H. Teuben, University of Groningen. Elemental analyses were carried out at the Analytical Department of the University of Groningen (compounds **1′**, **1**−**3**) and the University of Eindhoven (compounds **4**−**6**); quoted data are the average of at least two independent measurements. Silsesquioxane starting materials (*c*-$C_5H_9)_7Si_7O_9(OH)_3$,[14] (*c*-$C_5H_9)_7Si_7O_9(OSiMe_3)(OH)_2$,[14] (*c*-$C_5H_9)_7Si_7O_9(OSiMe_2C(H)CH_2)(OH)_2$,[52] (*c*-$C_5H_9)_7Si_7O_9(OSiMePh_2)(OH)_2$,[41] (*c*-$C_7H_{13})_6Si_6O_5(OH)_4$,[53] and (*c*-$C_5H_9)_7Si_8O_{12}(OH)$[13] were prepared following the referenced literature procedures.

(*c*-$C_5H_9)_7Si_7O_9(OSiMe_3)O_2SiCl_2$ (1). To a solution of (*c*-$C_5H_9)_7Si_7O_9(OSiMe_3)(OH)_2$ (20.40 g, 21.53 mmol) and 1 equiv of $SiCl_4$ (21.53 mmol, 2.47 mL) in 200 mL of hexanes, was added slowly 2 equiv of NEt_3 (0.04 mol, 6.00 mL). The resulting suspension was stirred overnight at ambient temperature to complete the reaction. Filtration and removal of the solvent afforded analytically pure **1** as a white powder (19.89 g, 17.40 mmol, 81%). ^{1}H NMR ($CDCl_3$): δ 0.18 (s, (CH_3)$_3$Si, 9H), 0.88−1.14 (m, CH−C_5H_9Si, 7H), 1.59 (m, CH_2−C_5H_9-Si, 42H), 1.79 (m, CH_2−C_5H_9, 14H). ^{13}C{^{1}H} NMR ($CDCl_3$): δ 1.74 ((*C*H$_3$)$_3$Si), 21.96, 22.23, 22.84, 22.95, 24.15 (1:1:2:2:1, *C*H−C_5H_9-Si), 26.92−27.62 (*C*H$_2$−C_5H_9Si). ^{29}Si NMR ($CDCl_3$): δ 9.34 (O*Si*Me$_3$), −64.97, −65.17, −66.32, −66.75, −67.85 (1:1:2:1:2, O_3*Si*C_5H_9), −69.42 (O_2*Si*Cl_2). IR (cm^{-1}, DuraSamplIR): 2948 (s), 2865 (m), 1449 (w), 1248 (m), 1080 (s), 951 (m), 911 (m), 832 (m), 786 (m), 720 (m). T_{mp}: 120 ± 2 °C. Elemental analysis calcd (%) for $C_{38}H_{72}Cl_2O_{12}Si_9$ (1044.66): C, 43.69; H, 6.95; Cl, 6.79. Found: C, 43.78; H, 6.98; Cl, 6.89.

(*c*-$C_6H_{11})_7Si_7O_9(OSiMe_3)O_2SiCl_2$ (1′). The cyclohexyl-substituted analogue of **1** was prepared following the same synthetic procedures and was isolated in 84% yield. Colorless crystals could be obtained from hexane, suitable for a single-crystal structure determination. ^{1}H NMR (C_6D_6): δ 0.36 (s, (CH_3)$_3$Si, 9H), 0.94−1.05 (m, CH−C_6H_{11}Si, 7H), 1.23 (m, CH_2−C_6H_{11}Si, 21H), 1.64 (m, CH_2−C_6H_{11}, 35H), 2.07 (m, CH_2−C_6H_{11}, 14H). ^{13}C{^{1}H} NMR (C_6D_6): δ 2.05 ((*C*H$_3$)$_3$Si), 23.46, 23.66, 24.01, 24.75, 25.42 (1:1:2:2:1, *C*H−C_6H_{11}Si), 26.88−28.01 (*C*H$_2$−C_5H_9Si). ^{29}Si NMR (C_6D_6): δ 10.49 (O*Si*Me$_3$), −66.16, −66.39, −67.39, −67.83, −69.24 (1:1:2:1:2, O_3*Si*C_6H_{11}), −67.74 (O_2*Si*Cl_2). T_{mp}: 167 ± 1 °C. Elemental analysis calcd (%) for $C_{45}H_{86}Cl_2O_{12}Si_9$ (1142.80): C, 47.29; H, 7.59; Cl, 6.20. Found: C, 47.35; H, 7.61; Cl, 6.26.

(*c*-$C_5H_9)_7Si_7O_9(OSiMe_2C(H)CH_2)O_2SiCl_2$ (2). Using the same procedure as for **1**, compound **2** was isolated as a white powder in 87% yield. ^{1}H NMR ($CDCl_3$): δ 0.25 (s, (CH_3)$_2$−Si−vinyl, 6H), 0.89−1.15 (m, CH−C_5H_9Si, 7H), 1.58 (m, CH_2−C_5H_9Si, 42H), 1.80 (m, CH_2−C_5H_9, 14H), 5.76−5.83 (dd, ^3J = 20.2 Hz, ^2J = 3.8 Hz, 1H, *trans*-SiCHCH_2), 5.94−5.99 (dd, ^3J = 14.9 Hz, ^2J = 3.8 Hz, 1H, *cis*-SiCHCH_2), 6.16−6.25 (dd, ^3J = 20.2 Hz, ^3J = 14.9 Hz, 1H, SiCHCH$_2$). ^{13}C{^{1}H} NMR ($CDCl_3$): δ 0.17 ((*C*H$_3$)$_2$−Si−vinyl), 21.94, 22.22, 22.28, 22.93, 24.07 (1:1:2:2:1, *C*H−C_5H_9Si), 26.90−27.58 (*C*H$_2$−C_5H_9-Si), 131.64 (CH*C*H$_2$SiMe$_2$), 139.20 (*C*HCH$_2$SiMe$_2$). ^{29}Si NMR ($CDCl_3$): δ −2.21 (O*Si*Me$_2$vinyl), −64.96, −65.16, −66.31, −66.61, −67.81 (1:1:2:1:2, O_3*Si*C_5H_9), −69.39 (O_2*Si*Cl_2). IR (cm^{-1}, DuraSamplIR): 2948 (s), 2864 (m), 1450 (w), 1249 (m), 1060 (s), 950 (m), 911 (m), 832 (m), 787 (m), 719 (w). T_{mp}: 118 ± 2 °C. Elemental analysis calcd (%) for $C_{39}H_{72}Cl_2O_{12}Si_9$ (1056.67): C, 44.33; H, 6.87; Cl, 6.71. Found: C, 44.31; H, 6.96; Cl, 6.69.

(*c*-$C_5H_9)_7Si_7O_9(OSiPh_2Me)O_2SiCl_2$ (3). Using the same procedure as for **1**, compound **3** was isolated as a white, extremely viscous oil in 84% yield. ^{1}H NMR ($CDCl_3$): δ 0.72 (s, (CH_3)SiPh_2, 3H), 0.84−1.17 (m, CH−C_5H_9Si, 7H), 1.53 (m, CH_2−C_5H_9Si, 42H), 1.80 (m, CH_2−C_5H_9, 14H), 7.38 (m, CH−Ph, 6H), 7.63 (m, CH−Ph, 4H). ^{13}C{^{1}H} NMR ($CDCl_3$): δ −0.59 (*C*H$_3$−SiPh$_2$), 21.95, 22.25, 22.33, 22.90, 23.96 (1:1:2:2:1, *C*H−C_5H_9Si), 26.89−27.49 (*C*H$_2$−C_5H_9Si), 127.52 (*m*-*C*$_6$H$_5$), 129.90 (*p*-*C*$_6$H$_5$), 134.08 (*o*-*C*$_6$H$_5$), 137.71 (*ipso*-*C*$_6$H$_5$). ^{29}Si NMR ($CDCl_3$): δ −0.73 (O*Si*MePh$_2$), −65.68, −65.97, −66,47, −66.52 (1:1:2:3, O_3*Si*C_5H_9), −67.81 (O_2*Si*Cl_2). IR (cm^{-1}, DuraSamplIR): 2948 (s), 2864 (s), 1451 (w), 1249 (m), 1085 (s), 911 (m), 799 (m), 739 (m), 718 (m). T_{mp}: not detected. Elemental analysis calcd (%) for $C_{48}H_{76}Cl_2O_{12}Si_9$ (1168.80): C 49.33, H 6.55, Cl 6.07, found C 49.44, H 6.73, Cl 5.47.

(*c*-$C_5H_9)_7Si_7O_9(OSiMe_3)O_2Si(OH)_2$ (4). Compound **1** was hydrolyzed by adding 1 mL of distilled water to a solution of **1** (5.0 g, 4.79 mmol) in THF. After being stirred at room temperature for 30 min, the volatiles were removed in vacuo. The remaining sticky white solid was dissolved in toluene (2 × 20 mL) and subsequently pumped to dryness. The same procedure was repeated with hexanes (20 mL), leaving **4** as a free-flowing white powder. Recrystallization from hexanes at −20 °C afforded analytically pure **4** (3.09 g, 3.07 mmol, 64%). ^{1}H NMR ($CDCl_3$): δ 0.21 (s, (CH_3)$_3$Si, 9H), 1.02 (m, CH−C_5H_9Si, 7H), 1.57 (m, CH_2−C_5H_9Si, 42H), 1.79 (m, CH_2−C_5H_9, 14H), 2.41 (s, Si(O*H*)$_2$, 1H), 3.80 (s, Si(O*H*)$_2$, 1H). ^{13}C{^{1}H} NMR ($CDCl_3$): δ 1.71 ((*C*H$_3$)$_3$Si), 22.10, 22.19, 22.43, 22.85, 24.21 (1:1:2:2:1, *C*H−C_5H_9Si), 26.95−27.52 (*C*H$_2$−C_5H_9Si). ^{29}Si NMR ($CDCl_3$): δ 11.21 (O*Si*Me$_3$), −64.81, −65.12, −65.38, −66.38, −67.33 (1:1:1:2:2, O_3*Si*C_5H_9), −89.43 (O_2*Si*(OH)$_2$). IR (cm^{-1}, DuraSamplIR, ν_{SiOH} from Nujol mull): 3515 (ν_{SiOH}, m), 3402 (ν_{SiOH}, m), 2949 (s), 2865 (s), 1445 (w), 1252 (m), 1083 (s), 953 (m), 911 (m), 844 (s), 758 (m). T_{mp}: 154 ± 0.5 °C. Elemental analysis calcd (%) for $C_{38}H_{74}O_{14}Si_9$ (1007.77): C, 45.29; H, 7.40. Found: C, 45.01; H, 7.21.

(*c*-$C_5H_9)_7Si_7O_9(OSiMe_2C(H)CH_2)O_2Si(OH)_2$ (5). Using the same procedure as for **4**, compound **5** was isolated as a white powder in 71% yield. ^{1}H NMR ($CDCl_3$): δ 0.28 (s, (CH_3)$_2$−Si−vinyl, 6H), 1.02 (m, CH−C_5H_9Si, 7H), 1.58 (m, CH_2−C_5H_9Si, 42H), 1.79 (m, CH_2−C_5H_9, 14H), 2.37 (br s, Si(O*H*)$_2$, 1H), 3.63 (br s, Si(O*H*)$_2$, 1H), 5.79−5.85 (dd, ^3J = 20.4 Hz, ^2J = 3.8 Hz, 1H, *trans*-SiCHCH_2), 5.94−5.99 (dd, ^3J = 14.7 Hz, ^2J = 3.8 Hz, 1H, *cis*-SiCHCH_2), 6.16−6.25 (dd, ^3J = 20.4 Hz, ^3J = 14.7 Hz, 1H, SiCHCH$_2$). ^{13}C{^{1}H} NMR ($CDCl_3$): δ 0.00 ((*C*H$_3$)$_2$Sivinyl), 22.08, 22.19, 22.44, 22.84, 24.09 (1:1:2:2:1, *C*H−C_5H_9Si), 26.93−27.49 (*C*H$_2$−C_5H_9Si), 132.30 (CH*C*H$_2$SiMe$_2$), 138.97 (*C*HCH$_2$SiMe$_2$). ^{29}Si NMR ($CDCl_3$): δ −0.70 (O*Si*Me$_2$vinyl), −64.98, −65.10, −65.36, −66.41, −67.39 (1:1:1:2:2, O_3*Si*C_5H_9), −89.45 (O_2*Si*(OH)$_2$). IR (cm^{-1}, DuraSamplIR, ν_{SiOH} from Nujol mull): 3520 (ν_{SiOH}, m), 3402 (ν_{SiOH}, m), 2948 (s), 2864 (s), 1450 (w), 1245 (m), 1082 (s), 951 (m), 911 (m), 865 (w), 832 (m), 790 (m). T_{mp}: 135 ± 0.5 °C. Elemental analysis calcd (%) for $C_{39}H_{74}O_{14}Si_9$ (1019.78): C, 45.93; H, 7.31. Found: C, 45.59; H, 7.31.

(*c*-$C_5H_9)_7Si_7O_9(OSiPh_2Me)O_2Si(OH)_2$ (6). Using the same procedure as for **4**, compound **6** was isolated as a white free- flowing powder in 78% yield. ^{1}H NMR ($CDCl_3$): δ 0.73 (s, (CH_3)−SiPh$_2$, 3H), 1.05 (m, CH−C_5H_9Si, 7H), 1.54 (m, CH_2−C_5H_9Si, 42H), 1.80 (m, CH_2−C_5H_9, 14H), 2.12 (s, Si(O*H*)$_2$, 1H), 2.23 (s, Si(O*H*)$_2$, 1H), 7.41 (m, CH−Ph, 6H), 7.68 (m, CH−Ph, 4H). ^{13}C{^{1}H} NMR ($CDCl_3$): δ −0.78 (*C*H$_3$−SiPh$_2$), 22.06, 22.25, 22.58, 22.95, 23.91 (1:1:2:2:1, *C*H−C_5H_9-Si), 26.93−27.48 (*C*H$_2$−C_5H_9Si), 127.75 (*m*-*C*$_6$H$_5$), 129.62 (*p*-*C*$_6$H$_5$), 134.10 (*o*-*C*$_6$H$_5$), 137.56 (*ipso*-*C*$_6$H$_5$). ^{29}Si NMR ($CDCl_3$): δ −10.74 (O*Si*MePh$_2$), −65.05, −65.28, −65.84, −66.37, −67.53 (1:1:1:2:2, O_3*Si*C_5H_9), −89.46 (O_2*Si*(OH)$_2$). IR (cm^{-1}, DuraSamplIR, ν_{SiOH} from Nujol mull): 3582 (ν_{SiOH}, m), 3438 (ν_{SiOH}, m), 2947 (s), 2864 (s), 1450 (w), 1245 (m), 1088 (s), 911 (m), 871 (w), 795 (m), 730 (m), 696 (m). T_{mp}: 138 ± 0.5 °C. Elemental analysis calcd (%) for $C_{48}H_{78}O_{14}Si_9$ (1131.91): C, 50.93; H, 6.95. Found: C, 49.87; H, 6.95.

(52) Wada, K.; Bundo, M.; Nakabayashi, D.; Itayama, N.; Kondo, T.; Mitsudo, T. *Chem. Lett.* **2000**, 628−629.
(53) Feher, F. J.; Budzichowski, T. A.; Blanski, R. L.; Weller, K. J.; Ziller, J. W. *Organometallics* **1991**, *10*, 2526−2528.

[(*c*-C_5H_9)$_7$$Si_7O_9$($OSiMePh_2$)($O_2$Si(OH)-)]$_2$-($\mu$-O) (7). A saturated *n*-heptane (10 mL) solution of compound **6** (1.0 g, 0.88 mmol) was left overnight at room temperature and subsequently stored at −5 °C. After several days, the thermodynamically stable condensed product **7** could be isolated in almost quantitative yield. Recrystallization from *n*-heptane afforded **7** as colorless crystals (0.3 g, 0.13 mmol, 15%) suitable for a single-crystal X-ray analysis. ^{1}H NMR ($CDCl_3$): δ 0.76 (s, (CH_3)−$SiPh_2$, 6H), 0.96 (m, CH−C_5H_9Si, 14H), 1.51 (m, CH_2−C_5H_9Si, 84H), 1.71 (m, CH_2−C_5H_9, 28H), 7.38 (m, CH−Ph, 12H), 7.63 (m, CH−Ph, 8H). ^{13}C{^{1}H} NMR ($CDCl_3$): δ −0.84 (*C*H$_3$−$SiPh_2$), 21.95, 22.37, 22.89, 23.04, 23.88 (1:1:2:2:1, *C*H−C_5H_9Si), 26.95−27.49 (*C*H$_2$−C_5H_9Si), 127.57 (*m*-C_6H_5), 129.31 (*p*-C_6H_5), 134.23 (*o*-C_6H_5), 137.88 (*ipso*-C_6H_5). ^{29}Si NMR ($CDCl_3$): δ −10.26 (O*Si*$MePh_2$), −65.00, −65.04, −65.82, −66.11, −67.85 (1:1:2:1:2, O_3*Si*C_5H_9), −97.76 (O_3*Si*(OH)). IR (cm^{-1}, ν_{SiOH} from Nujol mull): 3631 (ν_{SiOH}, m), 2948 (s), 2864 (s), 1450 (m), 1246 (m), 1104 (s), 1072 (s), 1025 (s), 943 (m), 911 (m), 791 (m), 731 (m), 697 (m). T_{mp}: 197 ± 1 °C. Elemental analysis calcd (%) for $C_{96}H_{154}O_{27}Si_{18}$ (2245.81): C, 51.34; H, 6.91. Found: C, 50.68; H, 6.84.

X-ray Crystal Structure Analysis of 1′. A suitable crystal was selected, mounted on a thin, glass fiber using paraffin oil, and cooled to the data collection temperature. Data were collected on a Bruker AXS SMART 1K CCD diffractometer using 0.3° ω-scans at 0, 90, and 180° in ϕ. Initial unit cell parameters were determined from 60 data frames collected at different sections of the Ewald sphere. Semiempirical absorption corrections based on equivalent reflections were applied.[54]

Systematic absences in the diffraction data and unit cell parameters were uniquely consistent with the reported space group. The structure was solved by direct methods, completed with difference Fourier syntheses, and refined with full-matrix least-squares procedures based on F^2. A hexane molecule was cocrystallized in the asymmetric unit. All hydrogen atoms were treated as idealized contributions. All scattering factors are contained in the SHELXTL 6.12 program library.[55]

X-ray Crystal Structure Analysis of 7. A colorless crystal measuring 0.18 × 0.12 × 0.06 mm was mounted under the cold nitrogen stream (150 K) on a Bruker[56] SMART APEX CCD diffractometer equipped with a 4K CCD detector set 60.0 mm from the crystal (Platform with full three-circle goniometer). Intensity data were corrected for Lorentz and polarization effects, scale variation, and decay and absorption: a multiscan absorption correction was applied, based on the intensities of symmetry-related reflections measured at different angular settings (SADABS),[57] and reduced to F_o^2. The program suite SHELXTL was used for space group determination (XPREP).[56] The structure was solved by Patterson methods, and extension of the model was accomplished by direct methods applied to difference structure factors using the program DIRDIF.[58] All refinement calculations were performed using the program packages SHELXL[59] and PLATON.[60]

Acknowledgment. This work was financially supported by the Dutch Polymer Institute (R.D.) and the Spinoza Fond, awarded to R.A.v.S.

Supporting Information Available: Experimental procedures and details of the structure determination, including tables of refined parameters, fractional atomic parameters, bond distances and angles, and torsion angles for **1′** and **7** (PDF). This material is available free of charge via the Internet at http://pubs.acs.org.

JA0122243

(54) Blessing, R. *Acta Crystallogr*. **1995**, *A51*, 33−38.
(55) Sheldrick, G. M., Bruker AXS, Madison, WI, 2001.
(56) Bruker 2000. SMART, SAINT, SADABS, XPREP, and SHELXTL/NT. Area Detector Control and Integration Software. Smart Apex Software Reference Manuals, Bruker Analytical X-ray Instruments. Inc., Madison, WI, 2000.
(57) Sheldrick, G. M. *Multi-Scan Absorption Correction Program*; University of Göttingen, Germany, 2000.
(58) Beurskens, P. T.; Beurskens, G.; de Gelder, R.; García-Granda, S.; Gould, R. O.; Israël, R.; Smits, J. M. M. *The DIRDIF-99 program system*; Crystallography Laboratory, University of Nijmegen, The Netherlands, 1999.
(59) Sheldrick, G. M. *Program for the Refinement of Crystal Structures*; University of Göttingen, Germany, 1997.
(60) Spek, A. L. *Program for the automated Analysis of Molecular Geometry* (A multipurpose Crystallographic Tool); University of Utrecht, The Netherlands, 2000.